L-SYSTEMS: FROM THE THEORY TO VISUAL MODELS OF PLANTS

Przemyslaw Prusinkiewicz†, Mark Hammel†,
Jim Hanan‡, and Radomír Měch†

†Department of Computer Science
University of Calgary
Calgary, Alberta, Canada T2N 1N4
e-mail: pwp|hammel|mech@cpsc.ucalgary.ca

‡CSIRO - Cooperative Research Centre for
Tropical Pest Management
Brisbane, Australia
e-mail: jim@ctpm.uq.oz.au

From M. T. Michalewicz, editor, *Proceedings of the 2nd CSIRO Symposium on Computational Challanges in Life Sciences*, CSIRO Publishing, 1996. To appear.

— CSIRO —
2nd CSIRO Symposium on Computational Challanges in Life Sciences

L-SYSTEMS: FROM THE THEORY TO VISUAL MODELS OF PLANTS

PRZEMYSLAW PRUSINKIEWICZ†
JIM HANAN‡

MARK HAMMEL†
RADOMIR MECH†

†*Department of Computer Science,*
University of Calgary
Calgary, Alberta T2N 1N4, Canada
e-mail: pwp|hammel|mech@cpsc.ucalgary.ca

‡*CSIRO - Cooperative Research Centre*
for Tropical Pest Management
Brisbane, Australia
e-mail: jim@ctpm.uq.oz.au

ABSTRACT

Recent advances in computer graphics have made it possible to visualize mathematical models of biological structures and processes with unprecedented realism. The resulting images, animations, and interactive systems are useful as research and educational tools in developmental biology and ecology. Prospective applications also include computer-assisted landscape architecture, design of new varieties of plants, and crop yield prediction. In this paper we revisit foundations of the applications of L-systems to the modeling of plants, and we illustrate them using recently developed sample models.

Keywords: L-system, fractal, plant, modeling, simulation, realistic image synthesis, emergence, artificial life

1. Introduction

In 1968, Aristid Lindenmayer introduced a formalism for simulating the development of multicellular organisms, subsequently named L-systems [1]. This formalism was closely related to abstract automata and formal languages, and attracted the immediate interest of theoretical computer scientists. The vigorous development of the mathematical theory of L-systems was followed by its applications to the modeling of plants. These applications gained momentum after 1984, when Smith introduced state-of-the art computer graphics techniques to visualize the structures and processes being modeled [2]. Smith also attracted attention to the phenomenon of *data-base amplification*, or the possibility of generating complex structures from compact data sets, which is inherent in L-systems and forms the cornerstone of L-system applications to image synthesis. Subsequent developments (presented here from our personal perspective, without covering the fast-growing array of contributions from many other researchers) included:

- introduction of turtle interpretation of L-systems [3,4] and refinement of a programming language based on L-systems [5,6], which facilitated specification

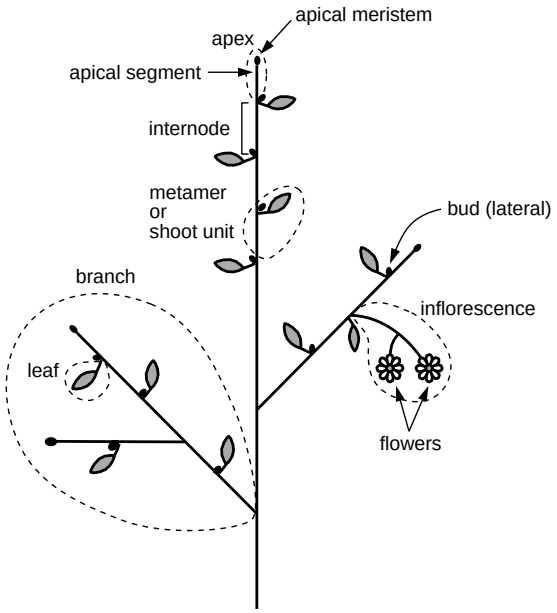

Figure 1: Selected modules and groups of modules (encircled with dashed lines) used to describe plants.

of the models for simulation purposes and promoted the use of L-systems as a language for describing models in publications;

- recognition of the fractal character of structures generated by L-systems, which related them to the dynamically developing science of fractals [3,6,7];
- increased interest in the application of computer simulations to the understanding of living processes and structures, related to the emergence of the field of Artificial Life;
- extension of the range of phenomena that can be modeled using L-systems, including, most recently, incorporation of environmental factors into the models [8,9];
- increased understanding of the modeling process, providing a methodology for constructing models according to biological observations and measurements [10,11].

In this paper, we revisit basic mechanisms that control plant development: lineage (cellular descent), captured by the class of context free L-systems, and endogenous interaction (transfer of information between neighboring modules in the structure), captured by context-sensitive L-systems (*c.f.* [12]). Within this framework, we present several models that have been developed after the most recent survey of L-systems [6].

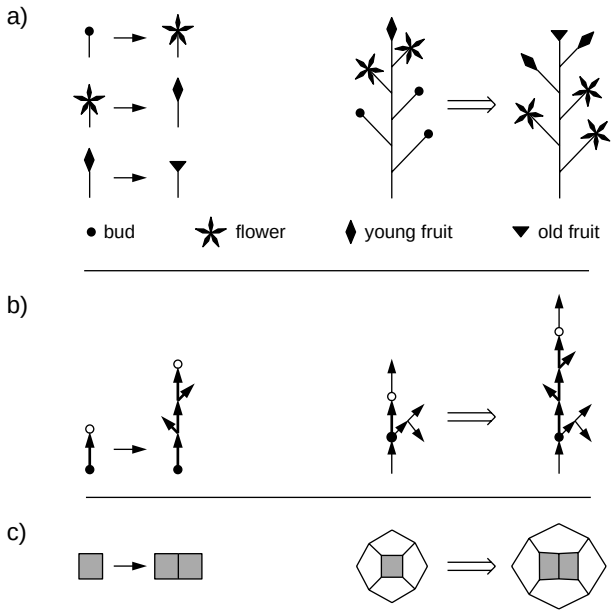

Figure 2: Examples of production specification and application: (a) development of a flower, (b) development of a branch, and (c) cell division.

2. The modular structure of plants

L-systems were originally introduced to model the development of simple *multicellular* organisms (for example, algae) in terms of division, growth, and death of individual cells [1,13]. The range of L-system applications has subsequently been extended to higher plants and complex branching structures, in particular inflorescences [14,15], described as configurations of modules in space. In the context of L-systems, the term *module* denotes any discrete constructional unit that is repeated as the plant develops, for example an internode, an apex, a flower, or a branch (Figure 1) [16,17,18]. The goal of modeling at the modular level is to describe the development of a plant as a whole, and in particular the emergence of plant shape, as the integration of the development of individual units.

3. Plant development as a rewriting process

The essence of development at the modular level can be conveniently captured by a parallel *rewriting system* that replaces individual *parent*, *mother*, or *ancestor* modules by configurations of *child*, *daughter*, or *descendant* modules. All modules belong to a finite *alphabet of module types*, thus the behavior of an arbitrarily large configuration of modules can be specified using a finite set of *rewriting rules* or *productions*. In the simplest case of *context-free* rewriting, a production consists of a single module called the *predecessor* or the *left-hand side*, and a configuration of zero, one, or more modules called the *successor* or the *right-hand side*. A production p with

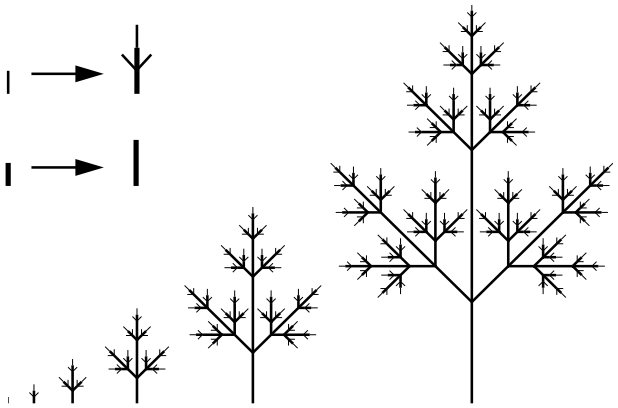

Figure 3: Developmental model of a compound leaf, modeled as a configuration of apices and internodes.

the predecessor matching a given mother module can be applied by deleting this module from the rewritten structure and inserting the daughter modules specified by the production's successor.

Three examples of production application are shown in Figure 2. In case (a), modules located at the extremities of a branching structure are replaced without affecting the remainder of the structure. In case (b), productions that replace internodes divide the branching structure into a lower part (below the internode) and an upper part. The position of the upper part is adjusted to accommodate the insertion of the successor modules, but the shape and size of both the lower and upper part are not changed. Finally, in case (c), the rewritten structures are represented by graphs with cycles. The size and shape of the production successor does not exactly match the size and shape of the predecessor, and the geometry of the predecessor and the embedding structure had to be adjusted to accommodate the successor. The last case is most complex, since the application of a local rewriting rule may lead to a global change of the structure's geometry. Developmental models of cellular layers operating in this manner have been presented in [6,19,20,21]. In this paper we focus on the rewriting of branching structures corresponding to cases (a) and (b).

Productions may be applied *sequentially*, to one module at a time, or they may be applied *in parallel*, with all modules being rewritten simultaneously in every *derivation step*. Parallel rewriting is more appropriate for the modeling of biological development, since development takes place simultaneously in all parts of an organism. A derivation step then corresponds to the progress of time over some interval. A sequence of structures obtained in consecutive derivation steps from a predefined *initial structure* or *axiom* is called a *developmental sequence*. It can be viewed as the result of a *discrete-time simulation* of development.

For example, Figure 3 illustrates the development of a stylized compound leaf including two module types, the *apices* (represented by thin lines) and the *internodes*

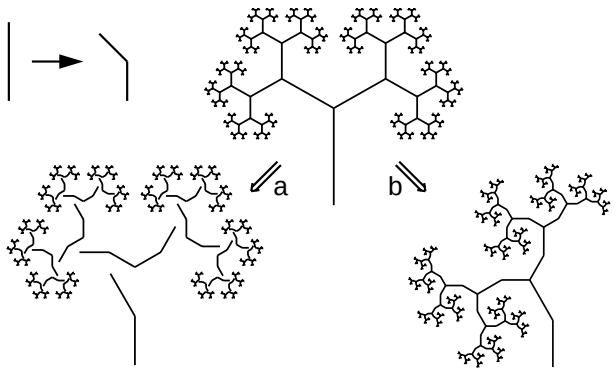

Figure 4: A comparison of the Koch construction (a) with a rewriting system preserving the branching topology of the modeled structures (b). The same production is applied in both cases, but the rules for incorporating the successor into the structure are different.

(thick lines). An apex yields a structure that consists of two internodes, two lateral apices, and a replica of the main apex. An internode elongates by a constant scaling factor. In spite of the simplicity of these rules, an intricate branching structure develops from a single apex over a number of derivation steps.

It is interesting to contrast simulation of development using rewriting rules with the well known Koch construction for generating fractals [22, page 39]. The essence of the Koch construction is the replacement of straight line segments by sets of lines. Their positions, orientations, and scales are determined by the position, orientation, and scale of the segment being replaced (Figure 4a). In contrast, in models of plants, the position and orientation of each module is determined by the chain of modules beginning at the base of the structure and extending to the module under consideration. For example, when the internodes bend, the subtended branches are rotated and displaced to maintain the connectivity of the structure (Figure 4b). Thus, development is simulated as a parallel application of productions, followed by a sequential connection of the child structures.

Rewriting processes maintaining the connectivity of branching structures can be defined directly in the geometric domain, but a more convenient approach is to express the generating rules and the resulting structures symbolically, using a string notation. A sequential geometric interpretation of these strings from the left (plant base) to right (branch extremities) automatically captures proper positioning of the higher branches on the lower ones. The rewriting of branching structures in the string domain is the cornerstone of L-systems.

The basic notions of the theory of L-systems have been presented in many survey papers [12,23,24,25,26,27] and books [6,7,28,29,30]. Consequently, we only describe parametric L-systems, which are a particularly convenient programming tool for expressing models of plant development. Our presentation closely follows the formalization introduced in [6,31] (see also [5,32]).

4. Parametric L-systems

Parametric L-systems operate on *parametric words*, which are strings of *modules* consisting of *letters* with associated *parameters*. The letters belong to an *alphabet* V, and the parameters belong to the set of *real numbers* $\Re$. A module with letter $A \in V$ and parameters $a_1, a_2, ..., a_n \in \Re$ is denoted by $A(a_1, a_2, ..., a_n)$. Every module belongs to the set $M = V \times \Re^*$, where $\Re^*$ is the set of all finite sequences of parameters. The set of all strings of modules and the set of all nonempty strings are denoted by $M^* = (V \times \Re^*)^*$ and $M^+ = (V \times \Re^*)^+$, respectively.

The real-valued *actual* parameters appearing in the words have a counterpart in the *formal* parameters, which may occur in the specification of L-system productions. If Σ is a set of formal parameters, then $C(\Sigma)$ denotes a *logical expression* with parameters from Σ, and $E(\Sigma)$ is an *arithmetic expression* with parameters from the same set. Both types of expressions consist of formal parameters and numeric constants, combined using the arithmetic operators $+$, $-$, $*$, $/$; the exponentiation operator $\wedge$, the relational operators $<$, $<=$, $>$, $>=$, $==$; the logical operators !, &&, || (not, and, or); and parentheses (). The expressions can also include calls to standard mathematical functions, such a natural logarithm, sine, floor, and functions returning random variables. The operation symbols and the rules for constructing syntactically correct expressions are the same as in the C programming language [33]. For clarity of presentation, however, we sometimes use Greek letters and symbols with subscripts in print. Relational and logical expressions evaluate to zero for false and one for true. A logical statement specified as the empty string is assumed to have value one. The sets of all correctly constructed logical and arithmetic expressions with parameters from Σ are noted $\mathcal{C}(\Sigma)$ and $\mathcal{E}(\Sigma)$.

A *parametric 0L-system* is defined as an ordered quadruple $G = \langle V, \Sigma, \omega, P \rangle$, where:

- V is the *alphabet* of the system,
- Σ is the *set of formal parameters*,
- $\omega \in (V \times \Re^*)^+$ is a nonempty parametric word called the *axiom*,
- $P \subset (V \times \Sigma^*) \times \mathcal{C}(\Sigma) \times (V \times \mathcal{E}(\Sigma)^*)^*$ is a finite *set of productions*.

The symbols : and $\rightarrow$ are used to separate the three components of a production: the *predecessor*, the *condition*, and the *successor*. Thus, a production has the format

$$pred : cond \rightarrow succ. \tag{1}$$

For example, a production with predecessor $A(t)$, condition $t > 5$ and successor $B(t+1)CD(t \wedge 0.5, t-2)$ is written as

$$A(t) : t > 5 \rightarrow B(t+1)CD(t \wedge 0.5, t-2). \tag{2}$$

A production in a 0L-system *matches* a module in a parametric word if the following conditions are met:

- the letter in the module and the letter in the production predecessor are the same,
- the number of actual parameters in the module is equal to the number of formal parameters in the production predecessor, and
- the condition evaluates to *true* if the actual parameter values are substituted for the formal parameters in the production.

A matching production can be *applied* to the module, creating a string of modules specified by the production successor. The actual parameter values are substituted for the formal parameters according to their position. For example, production (2) above matches a module $A(9)$, since the letter A in the module is the same as in the production predecessor, there is one actual parameter in the module $A(9)$ and one formal parameter in the predecessor $A(t)$, and the logical expression $t > 5$ is true for t equal to 9. The result of the application of this production is a parametric word $B(10)CD(3,7)$.

If a module a produces a parametric word χ as the result of a production application in an L-system G, we write $a \mapsto \chi$. Given a parametric word $\mu = a_1 a_2 ... a_m$, we say that the word $\nu = \chi_1 \chi_2 ... \chi_m$ is *directly derived* from (or *generated* by) μ and write $\mu \Longrightarrow \nu$ if and only if $a_i \mapsto \chi_i$ for all $i = 1, 2, ..., m$. A parametric word ν is generated by G in a *derivation of length* n if there exists a sequence of words $\mu_0, \mu_1, ..., \mu_n$ such that $\mu_0 = \omega$, $\mu_n = \nu$ and $\mu_0 \Longrightarrow \mu_1 \Longrightarrow ... \Longrightarrow \mu_n$.

An example of a parametric L-system is given below.

$$\begin{array}{lllll} \omega: & B(2)A(4,4) & & & \\ p_1: & A(x,y) & : y <= 3 & \rightarrow & A(x*2, x+y) \\ p_2: & A(x,y) & : y > 3 & \rightarrow & B(x)A(x/y, 0) \\ p_3: & B(x) & : x < 1 & \rightarrow & C \\ p_4: & B(x) & : x >= 1 & \rightarrow & B(x-1) \end{array} \tag{3}$$

It is assumed that a module replaces itself if no matching production is found in the set P. The words obtained in the first few derivation steps are shown in Figure 5.

Productions in parametric 0L-systems are *context-free*, *i.e.,* applicable regardless of the context in which the predecessor appears. A *context-sensitive* extension is necessary to model information exchange between neighboring modules. In general, a context-sensitive production has the format

$$lc < pred > rc : cond \rightarrow succ, \tag{4}$$

where symbols $<$ and $>$ separate the three components of the predecessor: a string of modules without brackets lc called the *left context*, a module *pred* called the *strict predecessor*, and a well-nested bracketed string of modules rc called the *right context*. The remaining components of the production are the condition *cond* and the successor *succ*, defined as for parametric 0L-systems.

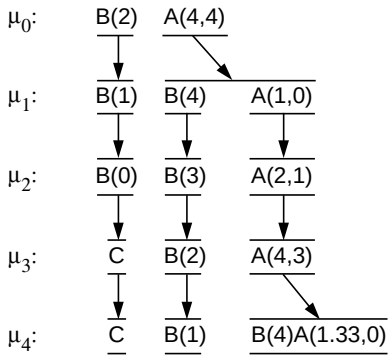

Figure 5: The initial sequence of strings generated by the parametric L-system specified in equation (3)

A sample context-sensitive production is given below:

$$A(x) < B(y) > C(z) : x + y + z > 10 \rightarrow E((x + y)/2)F((y + z)/2). \tag{5}$$

The left context is separated from the strict predecessor by the symbol $<$. Similarly, the strict predecessor is separated from the right context by the symbol $>$. Production 5 can be applied to the module $B(5)$ that appears in a parametric word

$$\cdots A(4)B(5)C(6)\cdots \tag{6}$$

since the sequence of letters A, B, C in the production and in parametric word (6) are the same, the numbers of formal parameters and actual parameters coincide, and the condition $4 + 5 + 6 > 10$ is true. As a result of the production application, the module $B(5)$ will be replaced by a pair of modules $E(4.5)F(5.5)$. Naturally, the modules $A(4)$ and $C(6)$ will be replaced by other productions in the same derivation step.

Productions in 2L-systems use context on both sides of the strict predecessor. 1L-systems are a special case of 2L-systems in which context appears only on one side of the productions.

When no production explicitly listed as a member of the production set P matches a module in the rewritten string, we assume that an appropriate *identity production* belongs to P and replaces this module by itself. Under this assumption, a parametric L-system $G = \langle V, \Sigma, \omega, P\rangle$ is called *deterministic* if and only if for each module $A(t_1, t_2, \ldots, t_n) \in V \times \Re^*$ the production set includes exactly one matching production. Within this paper we only consider deterministic L-systems.

5. The turtle interpretation of L-systems

Strings generated by L-systems may be interpreted geometrically in many different ways. Below we outline the *turtle interpretation* of L-systems, introduced by Szilard and Quinton [4], and extended by Prusinkiewicz [3,34] and Hanan [5,35]. A

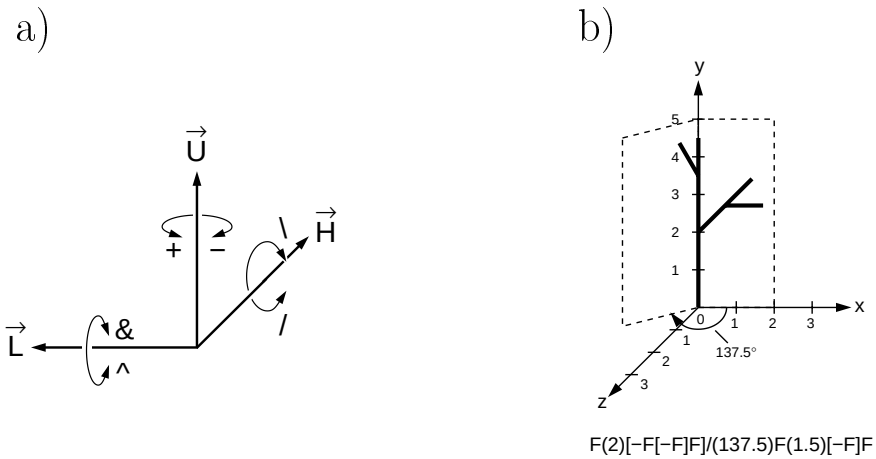

Figure 6: a) Controlling the turtle in three dimensions. b) Example of the turtle interpretation of a string.

tutorial exposition is included in [6], and subsequent results are presented in [5]. The summary below is based on [6,31,34,36].

After a string has been generated by an L-system, it is scanned sequentially from left to right, and the consecutive symbols are interpreted as commands that maneuver a LOGO-style turtle [37,38] in three dimensions. The turtle is represented by its *state*, which consists of turtle *position* and *orientation* in the Cartesian coordinate system, as well as various attribute values, such as current *color* and *line width*. The position is defined by a vector $\vec{P}$, and the orientation is defined by three vectors $\vec{H}$, $\vec{L}$, and $\vec{U}$, indicating the turtle's *heading* and the directions to the *left* and *up* (Figure 6a). These vectors have unit length, are perpendicular to each other, and satisfy the equation $\vec{H} \times \vec{L} = \vec{U}$. Rotations of the turtle are expressed by the equation:

$$\left[\begin{array}{ccc} \vec{H}' & \vec{L}' & \vec{U}' \end{array} \right] = \left[\begin{array}{ccc} \vec{H} & \vec{L} & \vec{U} \end{array} \right] \mathbf{R}, \tag{7}$$

where $\mathbf{R}$ is a 3×3 rotation matrix [39]. Changes in the turtle's state are caused by interpretation of specific symbols, each of which may be followed by parameters. If one or more parameters are present, the value of the first parameter affects the turtle's state. If the symbol is not followed by any parameter, default values specified outside the L-system are used. The following list specifies the basic set of symbols interpreted by the turtle.

Symbols that cause the turtle to move and draw

$F(s), G(s)$ Move forward a step of length s and draw a line segment from the original to the new position of the turtle.

$f(s), g(s)$ Move forward a step of length s without drawing a line.

$@O(r)$ Draw a sphere of radius r at the current position.

Symbols that control turtle orientation in space (Figure 6a)

$+(\theta)$ Turn left by angle θ around the $\vec{U}$ axis.

$-(\theta)$ Turn right by angle θ around the $\vec{U}$ axis.

$\&(\theta)$ Pitch down by angle θ around the $\vec{L}$ axis.

$\wedge(\theta)$ Pitch up by angle θ around the $\vec{L}$ axis.

$/(\theta)$ Roll left by angle θ around the $\vec{H}$ axis.

$\backslash(\theta)$ Roll right by angle θ around the $\vec{H}$ axis.

$|$ Turn 180° around the $\vec{U}$ axis. This is equivalent to $+(180)$ or $-(180)$.

Symbols for modeling structures with branches

[Push the current state of the turtle (position, orientation and drawing attributes) onto a pushdown stack.

] Pop a state from the stack and make it the current state of the turtle. No line is drawn, although in general the position and orientation of the turtle are changed.

Symbols for creating and incorporating surfaces

{ Start saving the subsequent positions of the turtle as the vertices of a polygon to be filled.

} Fill the saved polygon.

$\sim X(s)$ Draw the surface identified by symbol X, scaled by s, at the turtle's current location and orientation. Such a surface is usually defined as a bicubic patch [34,35].

Symbols that change the drawing attributes

$\#(w)$ Set line width to w, or increase the value of the current line width by the default width increment if no parameter is given.

$!(w)$ Set line width to w, or decrease the value of the current line width by the default width decrement if no parameter is given.

$;(n)$ Set the index of the color map to n, or increase the value of the current index by the default colour increment if no parameter is given.

$,(n)$ Set the index of the color map to n, or decrease the value of the current index by the default colour decrement if no parameter is given.

A sample string and its interpretation are shown in Figure 6b. The default length of lines represented by symbols F without a parameter is 1, and the default magnitude of the angles represented by symbols + and − is 45°.

6. Examples of parametric D0L-system models

This section presents selected examples that illustrate the operation of deterministic 0L-systems (D0L-systems) with turtle interpretation and their application to the modeling of plants. Many other examples are included in [5,6,31].

6.1. Fractal generation

Fractal curves provide a convenient means for illustrating the basic principle of L-system operation [3,6,7,40]. For example, the following L-system generates the well-known snowflake curve [22,41].

$$\begin{array}{ll} \omega & : \quad F(1) - (120)F(1) - (120)F(1) \\ p_1 & : \quad F(s) \rightarrow F(s/3) + (60)F(s/3) - (120)F(s/3) + (60)F(s/3) \end{array} \tag{8}$$

The axiom $F(1)-(120)F(1)-(120)F(1)$ draws an equilateral triangle, with edges of unit length. Production p_1 replaces each line segment with a polygonal shape, as shown at the top of Figure 7. Productions for symbols + and − are not listed, which means that the corresponding modules will be replaced by themselves during the derivation. The same effect could have been obtained by explicit inclusion of productions:

$$\begin{array}{ll} p_2 & : \quad +(a) \rightarrow +(a) \\ p_3 & : \quad -(a) \rightarrow -(a) \end{array} \tag{9}$$

The axiom and the figures obtained in the first three derivation steps are shown at the bottom of Figure 7.

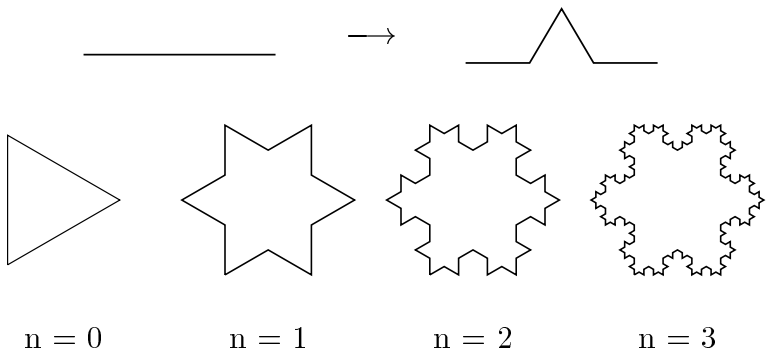

Figure 7: Visual interpretation of the production for the snowflake curve, and the curve after $n = 0$, 1, 2, and 3 derivation steps

6.2. Simulation of development

The next L-system generates the developmental sequence of the stylized compound leaf model presented in Figure 3.

$$\begin{array}{lll} \omega: & !(1)F(1,1) & \\ p_1: & F(s) \rightarrow & G(s)[-!(1)F(s)][+!(1)F(s)]G(s)!(1)F(s) \\ p_2: & G(s) \rightarrow & G(2*s) \\ p_3: & !(w) \rightarrow & !(3) \end{array} \tag{10}$$

The structure is built from two module types, apices F (represented by thin lines) and internodes G (thick lines). In both cases the parameter s determines the length of the line representing the module. An apex yields a structure that consists of two internodes, two lateral apices, and a replica of the main apex (production p_1). An internode elongates by a constant scaling factor (production p_2). Production p_3 is used to make the lines representing the internodes wider (3 units of width) than the lines representing the apices (1 unit). The branching angle associated with symbols $+$ and $-$ is set to 45° by a global variable outside the L-system.

6.3. Exploration of parameter space

Parametric L-systems provide a convenient mathematical framework for exploring the range of forms that can be captured by the same structural model with varying attributes (constants in the productions). Such *parameter space explorations* motivated some of the earliest computer simulations of biological structures: the models of sea shells devised by Raup and Michelson [42,43] and the models of trees proposed by Honda [44] to study factors that determine overall tree shape. Parameter space exploration may reveal an unexpected richness of forms that can be produced by even the simplest models. For example, Figure 8 shows nine branching structures selected from a continuum generated by the following parametric D0L-system:

$$\begin{array}{lll} \omega: & A(100, w_0) & \\ p_1: & A(s,w) & : s >= min \rightarrow !(w)F(s) \\ & & [+(\alpha_1)/(\varphi_1)A(s*r_1, w*q \wedge e)] \\ & & [+(\alpha_2)/(\varphi_2)A(s*r_2, w*(1-q) \wedge e)] \end{array} \tag{11}$$

The single non-identity production p_1 replaces apex A by an internode F and two new apices A. The angle values α_1, α_2, φ_1, and φ_2 determine the orientation of these apices with respect to the subtending internode. Parameters s and w specify internode length and width. The constants r_1 and r_2 determine the gradual decrease in internode length that occurs while traversing the tree from its base towards the apices. The constants w_0, q, and e control the width of branches. The initial stem width is specified by w_0 in the second parameter of the axiom module A. For $e = 0.5$, the combined area of the descendant branches is equal to the area of the

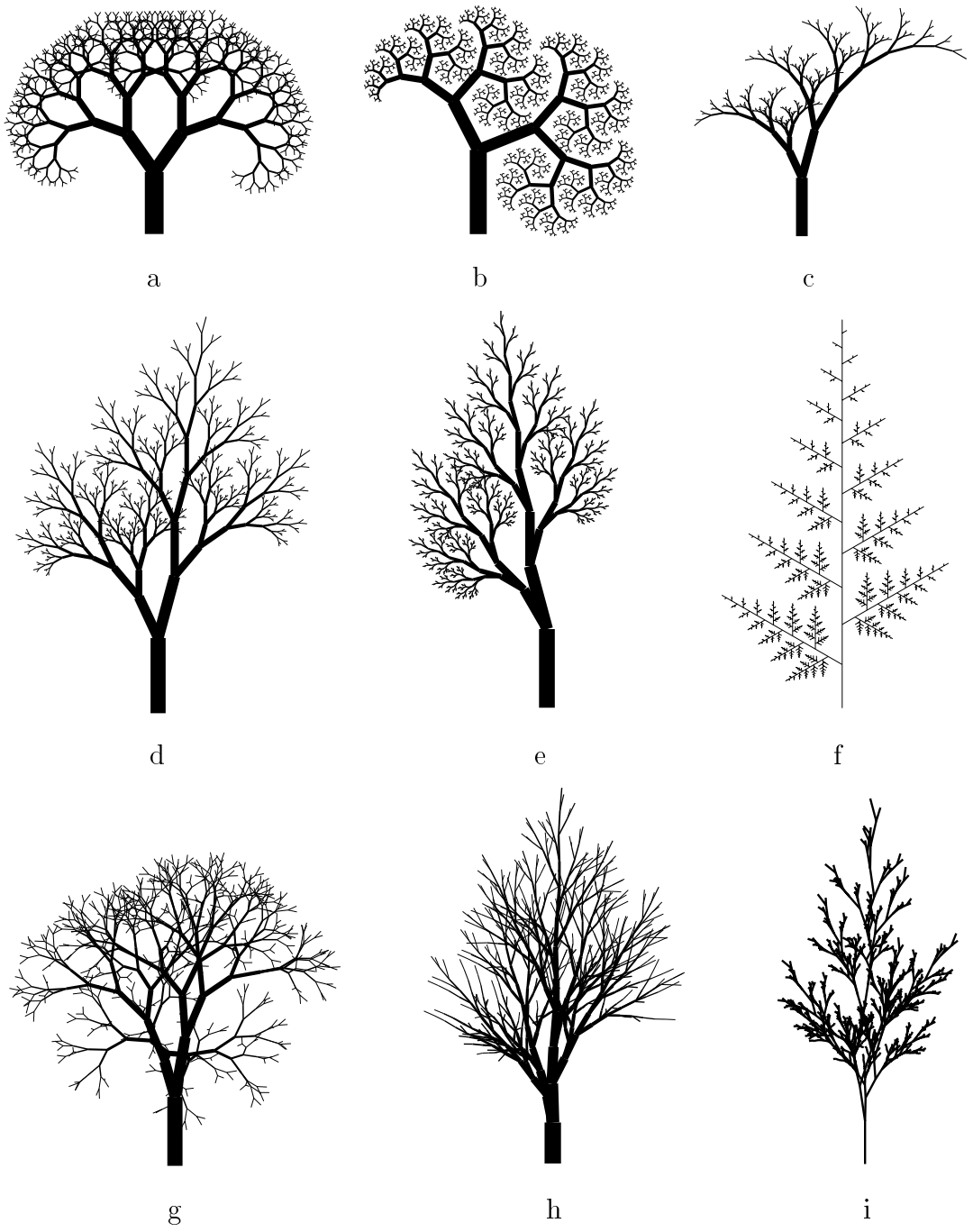

Figure 8: Sample structures generated by a parametric D0L-system with different values of constants

Table 1: The values of constants used to generate Figure 8

Figure	r_1	r_2	α_1	α_2	φ_1	φ_2	w_0	q	e	min	n
a	.75	.77	35	-35	0	0	30	.50	.40	0.0	10
b	.65	.71	27	-68	0	0	20	.53	.50	1.7	12
c	.50	.85	25	-15	180	0	20	.45	.50	0.5	9
d	.60	.85	25	-15	180	180	20	.45	.50	0.0	10
e	.58	.83	30	15	0	180	20	.40	.50	1.0	11
f	.92	.37	0	60	180	0	2	.50	.00	0.5	15
g	.80	.80	30	-30	137	137	30	.50	.50	0.0	10
h	.95	.75	5	-30	-90	90	40	.60	.45	25.0	12
i	.55	.95	-5	30	137	137	5	.40	.00	5.0	12

mother branch, as postulated by Leonardo da Vinci [22, page 156] (see also [45, pages 131–135]). The value q specifies the differences in width between descendant branches originating at the same vertex. Finally, the condition prevents formation of branches with length less then the threshold value *min*. The values of constants corresponding to each structure are collected in Table 1. The final column headed n indicates the number of derivation steps.

6.4. Modeling mesotonic and acrotonic structures

In spite of their apparent diversity, the structures generated by L-system (11) share a common developmental pattern: in each derivation step, every apex gives rise to an internode terminated by a pair of new apices. This is a simple instance of *subapical branching*, a common developmental pattern in plants, in which new branches are initiated only near the apices of the existing axes. As a consequence of this pattern, the lower branches, being created first, have more time to develop than the branches further up, and a *basitonic* structure (more developed near the base than near the top) results (Figure 9a). In nature, however, one also finds *mesotonic* and *acrotonic* structures, in which the most developed branches are located near the middle or the top of the mother branch (Figures 9 b and c). As observed by Frijters

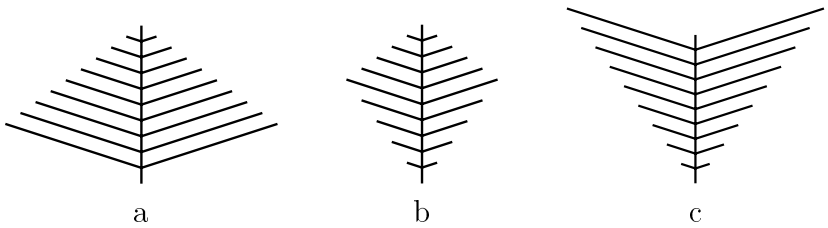

Figure 9: Schematic representation of a basitonic (a), mesotonic (b), and acrotonic (c) branching pattern. From [46].

and Lindenmayer [15], and formalized by Prusinkiewicz and Kari [46], arbitrarily large mesotonic and acrotonic structures cannot be generated by non-parametric deterministic 0L-systems with subapical branching. In contrast, *parametric* D0L-systems can generate such structures. For example, the following parametric D0L-system generates the mesotonic structure shown in Figure 9b.

$$\begin{array}{lll} \omega: & FA(0) & \\ p_1: & A(v) & \rightarrow [-FB(v)][+FB(v)]FA(v+1) \\ p_2: & B(v) : v > 0 & \rightarrow FB(v-1) \end{array} \tag{12}$$

The axiom ω defines the initial structure as an internode F terminated by an apex A. In each derivation step, the apex A adds a new segment F to the main axis and initiates a pair of branches FB (production p_1). The value of parameter v assigned to the lateral apices B describes the maximum length to which each branch will grow (production p_2). This value is incremented acropetally (*i.e.,* in the ascending order of branches) by production p_1, yielding a sequence of branches of increasing length. This sequence is broken in the upper part of the structure, where the branches still grow. Consequently, the younger branches near the top are shorter than the older ones further down, and a mesotonic overall structure results.

A detailed discussion of the generation of mesotonic and acrotonic structures using a construct similar to parametric L-systems has been presented by Lück, Lück, and Bakkali [47].

6.5. The shedding of branches

The natural processes of plant development often involve shedding, or programmed removal of selected modules from the growing structure. In order to simulate shedding, Hanan [5] extended the formalism of L-systems with the *cut symbol* %, which causes the removal of the remainder of the branch that follows it. For example, in the absence of other productions, the derivation step given below takes place:

$$a[b\%[cd]e[\%f]]g[h[\%i]j]k \Longrightarrow a[b]g[h[]j]k \tag{13}$$

A simple example of an L-system incorporating the cut symbol is given below:

$$\begin{array}{lllll} \omega: & A & & & \\ p_1: & A & & \rightarrow & F(1)[-X(3)B][+X(3)B]A \\ p_2: & B & & \rightarrow & F(1)B \\ p_3: & X(d) & : d > 0 & \rightarrow & X(d-1) \\ p_4: & X(d) & : d == 0 & \rightarrow & U\% \\ p_5: & U & & \rightarrow & F(0.3) \end{array} \tag{14}$$

According to production p_1, in each derivation step the apex of the main axis A produces an internode F of unit length and a pair of lateral apices B. Each apex B extends a branch by forming a succession of internodes F (production p_2). After

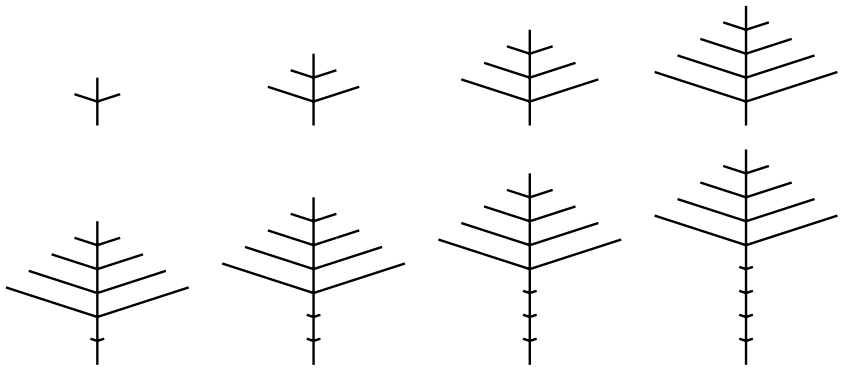

Figure 10: A developmental sequence generated by the L-system specified in Equation 14. The images shown represent derivation steps 2 through 9.

three steps from branch initiation (controlled by production p_3), production p_4 inserts the cut symbol % and an auxiliary symbol U at the base of the branch. In the next step, the cut symbol removes the branch, while symbol U inserts a marker $F(0.3)$ indicating a "scar" left by the removed branch. The resulting developmental sequence is shown in Figure 10. The initial steps capture the growth of a basitonic structure. Beginning at derivation step 6, the oldest branches are shed, creating an impression of a tree crown of constant shape and size moving upwards. The crown is in a state of dynamic equilibrium: the addition of new branches and internodes at the apices is compensated by the loss of branches further down.

The state of dynamic equilibrium can be easily observed in the development of palms, where new leaves are created at the apex of the trunk while old leaves are shed at the base of the crown (Figure 11). Since both processes take place at the same rate, an adult palm carries an approximately constant number of leaves. This phenomenon has an interesting physiological explanation: palms are unable to gradually increase the diameter of their trunk over time, thus the flow of water and nutrients through the trunk can support only a crown of constant size.

7. Examples of context-sensitive L-system models

In this section we consider the propagation of control information through the structure of the developing plant (*endogenous information flow* [48]), which is captured by context-sensitive productions in the framework of L-systems. The conceptual elegance and expressive power of context-sensitive productions are among the most important assets of L-systems in modeling applications.

7.1. Development of a mesotonic structure

As outlined in Section , arbitrarily large mesotonic and acrotonic structures cannot be generated using deterministic 0L-systems without parameters [46]. The

Figure 11: A model of the date palm (*Phoenix dactylifera*). This image was created using an L-system with the general structure specified in Equation 14.

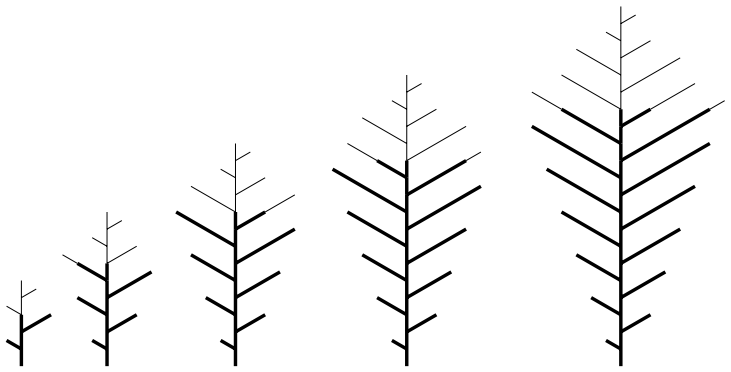

Figure 12: Development of a mesotonic branching structure controlled by an acropetal signal. Wide lines indicate the internodes reached by the signal. The stages shown correspond to derivation lengths 12, 24, 36, 48, and 60.

proposed mechanisms for modeling these structures can be divided into two categories: those using parameters to characterize the growth potential or vigor of individual apices, such as L-system (12), and those postulating control of development by signals [14,49]. The following L-system simulates the development of the mesotonic structure shown in Figure 12 using an acropetal (upward moving) signal.

$$
\begin{array}{lll}
\#\text{define} & m \;\; 3 & /* \text{ plastochron of the main axis } */ \\
\#\text{define} & n \;\; 4 & /* \text{ plastochron of the branch } */ \\
\#\text{define} & u \;\; 4 & /* \text{ signal propagation rate in the main axis } */ \\
\#\text{define} & v \;\; 2 & /* \text{ signal propagation rate in the branch } */
\end{array}
$$

$$
\text{ignore : } \; + - /
$$

$$
\begin{array}{ll}
\omega : & S(0)F(1,0)A(0) \\
p_1 : & A(i) \;\; : i < m-1 \rightarrow A(i+1) \\
p_2 : & A(i) \;\; : i == m-1 \rightarrow [+(60)F(1,1)B(0)]F(1,0)/(180)A(0) \\
p_3 : & B(i) \;\; : i < n-1 \rightarrow B(i+1) \\
p_4 : & B(i) \;\; : i == n-1 \rightarrow F(1,1)B(0) \\
p_5 : & S(i) \;\; : i < u+v \rightarrow S(i+1) \\
p_6 : & S(i) \;\; : i == u+v \rightarrow \varepsilon \\
p_7 : & S(i) < F(l,o) : (o == 0)\&\&(i == u-1) \rightarrow \#F(l,o)!S(0) \\
p_8 : & S(i) < F(l,o) : (o == 1)\&\&(i == v-1) \rightarrow \#F(l,o)!S(0) \\
p_9 : & S(i) < B(j) \rightarrow \varepsilon
\end{array}
\tag{15}
$$

L-system (15) operates under the assumption that the context-sensitive production p_9 takes priority over p_3 or p_4. The ignore statement lists symbols that should not be taken for consideration for context-matching purposes. The axiom ω describes the initial structure as an internode F terminated by an apex A. A signal S is placed at the base of this structure. According to productions p_1 and p_2, the apex

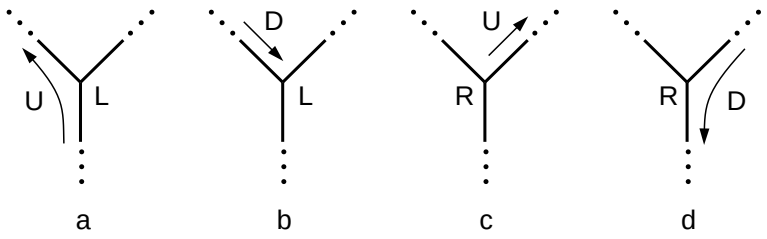

Figure 13: Insect's behavior at a branching point. An upward-moving insect U that approaches a branching point L is directed to the left daughter branch (a). A downward moving insect D that approaches a branching point marked L changes this marking to R, returns to state U, and enters the right branch (b and c). A downward moving insect D approaching a branching point R continues its downward motion (d).

A periodically produces a lateral branch and adds an internode to the main axis. The period (called the *plastochron* of the main axis) is controlled by the constant m. Productions p_3 and p_4 describe the development of the lateral branches, where new segments F are added with plastochron n. Productions p_5 to p_8 describe the propagation of the signal through the structure. The signal propagation rate is u in the main axis, and v in the branches. Production p_9 removes the apex B when the signal reaches it, thus terminating the development of the corresponding lateral branch. Figure 12 shows that, for the values of plastochrons and signal propagation rates specified be the #define statements, the lower branches have less time to grow than the higher branches, and a mesotonic structure develops as a result.

A similar mechanism, based on the pursuit of apices by acropetal signals, has been proposed to model basipetal flowering sequences [6,49,50]. These sequences are characterized by the appearance of the first flower near the top of a plant, and a subsequent downward propagation of the flowering zone.

7.2. Attack of a plant by an insect

More complex information flow is considered in the next example. A hypothetical insect explores a growing branching structure and feeds on its apices. The insect always moves along the branches (*i.e.,* it does not jump or drop from one branch to another) and therefore can be treated as an endogenous signal. The insect's behavior at a branching point depends on its direction of motion and the state of the branching point, as explained in Figure 13. In a nutshell, the insect attempts to traverse the entire developing structure using the depth-first strategy. A context-sensitive L-system that integrates plant growth with the behavior of the insect is given below.

```
#define l_L  3    /* length of the left branch */
#define l_R  5    /* length of the right branch */
#define d    5    /* plastochron */
#define w    40   /* delay */
```

$$
\begin{array}{lllll}
\omega & : & W(w)FA(l_L, d) & & \\
p_1 : & F & < \; A(n,m) & : m > 0 & \\
 & & & \rightarrow \; A(n, m-1) & \\
p_2 : & F & < \; A(n,m) & : n > 0 \;\&\&\; m == 0 & \\
 & & & \rightarrow \; FA(n-1, d) & \\
p_3 : & F & < \; A(n,m) & : n == 0 \;\&\&\; m == 0 & \\
 & & & \rightarrow \; L[+FA(l_L, d)][-FA(l_R, d)] & (16) \\
p_4 : & W(t) & : \; t > 0 & \rightarrow \; W(t-1) & \\
p_5 : & W(t) & : \; t == 0 & \rightarrow \; U & \\
p_6 : & U & < \; F & \rightarrow \; FU & \\
p_7 : & U & & \rightarrow \; \varepsilon & \\
p_8 : & UL & < \; + & \rightarrow \; +U & \\
p_9 : & U & < \; A(n,m) & \rightarrow \; D & \\
p_{10} : & F & > \; D & \rightarrow \; DF & \\
p_{11} : & D & & \rightarrow \; \varepsilon & \\
p_{12} : & L & > \; [+D] & \rightarrow \; UR & \\
p_{13} : & UR & < \; - & \rightarrow \; -U & \\
p_{14} : & R & > \; [\,][-D] & \rightarrow \; D &
\end{array}
$$

Productions p_1 to p_3 describe the development of a simple branching structure. Starting with a single axis specified by axiom ω, the apex A appends a sequence of branch segments F to the current axis (productions p_1 and p_2), then initiates a pair of new lateral apices (production p_3) that recursively repeat the same pattern. Parameter m is used to count the derivation steps between the creation of consecutive segments F. Parameter n determines the remaining number of segments to be produced before the next branching occurs. The total number of segments in an axis is defined by constants l_L (for the main axis and the branches issued to the left) and l_R (for the branches issued to the right). A newly created branching point is marked by symbol L (production p_3).

After a delay of w steps introduced by production p_4, production p_5 places an insect in the state U at the base of the branching structure. This insect moves upwards, one branch segment per derivation step (productions p_6 and p_7), until it encounters the branching point marker L. The insect is then directed to the left daughter branch (production p_8). After crossing a number of segments and, possibly, further branching points, the insect eventually reaches an apex A. As specified by production p_9, this apex is then removed from the structure, thus stopping further growth of its axis, and the state of the insect is changed from U (moving upwards) to D (moving downwards). The downward movement is simulated by productions

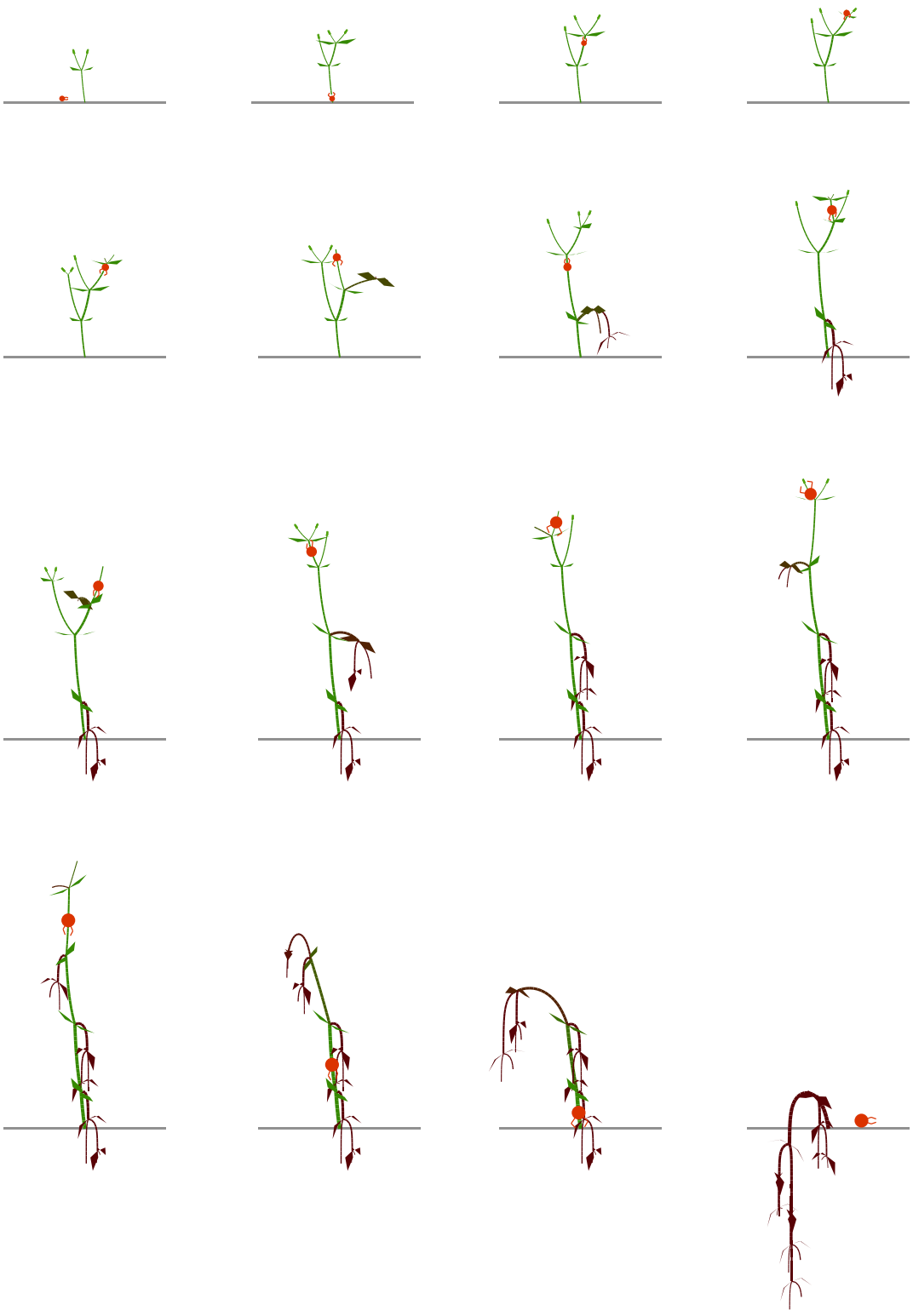

Figure 14: Simulation of the development of a plant attacked by an insect

p_{10} and p_{11}. Returning to a branching point marked L, the insect changes this mark to R to indicate that the left branch has been already explored, reverts its own state to U, and enters the right branch (productions p_{12} and p_{13}). Coming back from that branch, the insect continues its downward movement (production p_{14}) until it reaches another branching point marked L and enters an unexplored right branch, or until it completes the traversal of the entire structure at its base.

A sequence of images obtained using a straightforward extension of L-system (16) is shown in Figure 14. In this case, the insect feeds on the apices of a three-dimensional structure, and a branch that no longer carries any apices wilts.

Similar models can be constructed assuming different traversing and feeding strategies for one or many insects (which may interact with each other). Prospective applications of such models include simulation studies of insects used for weed control and of the impact of insects on crop plants [11,51].

7.3. Development controlled by resource allocation

In the previous examples, discrete information was transferred between the modules of a developing structure. A signal (or insect) was either present or absent at any particular point, and affected the structure in an "all-or-nothing" manner, by removing the apices at the ends of branches. In nature, however, developmental processes are often controlled in a more modulated way, by the quantity of substances (*resources*) exchanged between the modules. For example, the growth of plants depends on the amount of water and minerals absorbed by the roots and carried acropetally (upwards), and by the amount of photosynthates produced by the leaves and transported basipetally. An early developmental model of branching structures making use of quantitative information flow was proposed by Borchert and Honda [52]. Below we restate the essence of this model using the formalism of L-systems, then we extend it to simulate interactions between the shoot and the roots in a growing plant.

Borchert and Honda postulated that the development of a branching structure is controlled by a flow or *flux* of substances, which propagate from the base of the structure towards the apices and supply them with materials needed for growth. When the flux reaching an apex exceeds a predefined threshold value, the apex bifurcates and initiates a lateral branch; otherwise it remains inactive. At branching points the flux is distributed according to the types of the supported internodes (straight or lateral) and the number of apices in the corresponding branches. These numbers are accumulated by messages that originate at the apices and propagate towards the base of the plant. Thus, development is controlled by a cycle of alternating acropetal and basipetal information flow.

An L-system that implements these mechanisms is given below.

$$
\begin{array}{l}
\text{\#define } \alpha_1 \;\; 10 \;\; \text{/* branching angle - straight segment */} \\
\text{\#define } \alpha_2 \;\; 32 \;\; \text{/* branching angle - lateral segment */} \\
\text{\#define } \sigma_0 \;\; 17 \;\; \text{/* initial flux */} \\
\text{\#define } \eta \;\; 0.89 \text{ /* controls input flux changes */} \\
\text{\#define } \lambda \;\; 0.7 \;\; \text{/* flux distribution factor */} \\
\text{\#define } v_{th} \;\; 5.0 \;\; \text{/* threshold flux for branching */} \\
\\
\text{ignore: } + - / \\
\\
\omega \;:\; N(1)I(0,2,0,1)A \\
p_1 :\; N(k) < I(b,m,v,c) : b == 0 \;\&\&\; m == 2 \\
\qquad \rightarrow I(b,1,\sigma_0 * 2 \wedge (k-1) * (\eta \wedge k), c) \\
p_2 :\; N(k) > I(b,m,v,c) : b == 0 \;\&\&\; m == 2 \rightarrow N(k+1) \\
p_3 :\; I(b_l,m_l,v_l,c_l) < I(b,m,v,c) : m_l == 1 \;\&\&\; b == 1 \\
\qquad \rightarrow I(b,m_l,v_l - v_l * (1-\lambda) * ((c_l - c)/c), c) \\
p_4 :\; I(b_l,m_l,v_l,c_l) < I(b,m,v,c) : m_l == 1 \;\&\&\; b == 2 \\
\qquad \rightarrow I(b,m_l,v_l * (1-\lambda) * (c/(c_l - c)), c) \\
p_5 :\; I(b,m,v,c) < A : m == 1 \;\&\&\; v > v_{th} \\
\qquad \rightarrow /(180)[-(\alpha_2)I(2,2,v*(1-\lambda),1)A] \\
\qquad\quad +(\alpha_1)I(1,2,v*\lambda,1)A \\
p_6 :\; I(b,m,v,c) > A : m == 1 \;\&\&\; v <= v_{th} \rightarrow I(b,2,v,c) \\
p_7 :\; I(b,m,v,c) > [I(b_2,m_2,v_2,c_2) =] I(b_1,m_1,v_1,c_1) : \\
\qquad\quad m == 0 \;\&\&\; m_1 == 2 \;\&\&\; m_2 == 2 \\
\qquad \rightarrow I(b,2,v,c_1 + c_2) \\
p_8 :\; I(b,m,v,c) : m == 1 \rightarrow I(b,0,v,c) \\
p_9 :\; I(b_l,m_l,v_l,c_l) < I(b,m,v,c) : m_l == 2 \;\&\&\; m == 2 \\
\qquad \rightarrow I(b,0,v,c)
\end{array}
\tag{17}
$$

This L-system operates on three types of modules: apices A, internodes I, and an auxiliary module N. The internodes are visualized as lines of unit length. Each internode has four parameters:

- **segment type** b, where 0 denotes base of the tree, 1 – a straight segment, and 2 – a lateral segment;
- **message type** m, where 0 denotes no message currently carried by the internode, 1 – an acropetal message (flux), and 2 – a basipetal message (apex count);
- **flux value** v, and
- **apex count** c.

All internodes are visualized as lines of unit length.

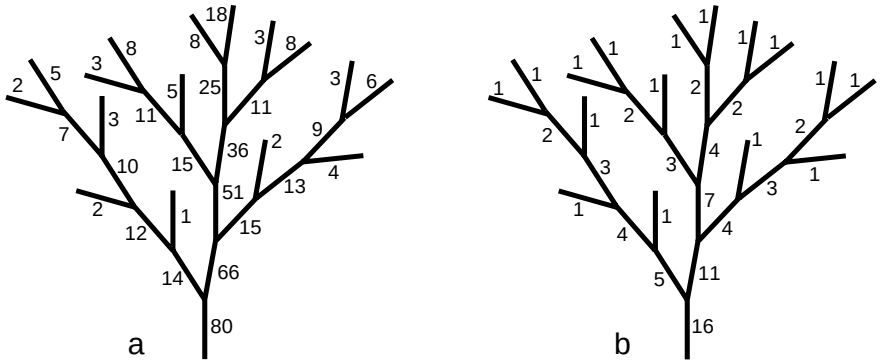

Figure 15: The structure generated by L-system (17) at completion of the fifth developmental cycle. The numbers indicate the flow values v rounded to the nearest integer (a), and the numbers of apices c in the branches supported by each internode (b).

At the beginning of a developmental cycle, indicated by the presence of a basipetal message ($m = 2$) in the basal internode ($b = 0$), production p_1 calculates an input flux value. The expression used for this purpose, $v = \sigma_0 2^{(k-1)\eta^k}$, was introduced by Borchert and Honda to simulate a sigmoid increase of flux penetrating the base of a plant over time. The progress of time is captured by production p_2, which increments the current cycle number k in module N.

Productions p_3 and p_4 simulate acropetal flux propagation and distribute it between the straight segment and the lateral segment. If both the straight and lateral branch support the same number of apices, the straight segment will obtain a predefined fraction λ of the flux v_l reaching the branching point; the lateral segment will obtain the remainder, $(1 - \lambda)v_l$. If a lateral branch supports c apices and its sister straight branch supports c_s apices, the flux reaching the lateral branch is further multiplied by the ratio c/c_s. The number c_s is not directly available to the lateral branch, but it can be calculated as the difference between the number of apices supported by this branch and its mother, $c_s = c_l - c$. In total, the flux directed towards the lateral branch is equal to $v_l(1 - \lambda)(c/(c_l - c)$ (production p_3). The remaining flux reaches the straight segment. The parameter c denotes, in this case, the number of apices supported by the straight segment, and the resulting expression is $v_l - v_l(1 - \lambda)((c_l - c)/c)$ (production p_4).

Productions p_5 and p_6 control the addition of new segments to the structure. According to production p_5, if the internode preceding an apex A reaches a sufficient flux $v > v_{th}$, the apex will create two new internodes I terminated by apices A. The new segments are assigned an initial message type $m = 2$, which triggers the basipetal signal propagation needed to update the count of apices supported by each segment. Alternatively, if the flux reaching an apex is not sufficient for bifurcation ($v \leq v_{th}$), the supporting internode itself starts the propagation of the basipetal signal (production p_6).

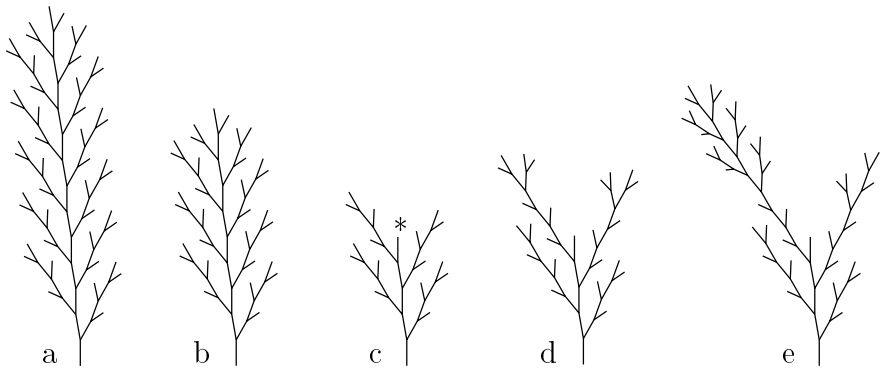

Figure 16: Development of a branching structure simulated using an L-system implementation of the model by Borchert and Honda. (a) Development not affected by pruning; (b, c) the structure immediately before and after pruning; (d, e) the subsequent development of the pruned structure. Based on [52].

Production p_7 adds the number of apices supported by the daughter branches (c_1 and c_2), and propagates the result to the mother internode. Both input numbers must be available ($m_1 = 2$ and $m_2 = 2$) before basipetal message propagation takes place.

The remaining productions reset the message value m to zero, after the flux values have been transferred acropetally (p_8) or the apex count has been passed basipetally (p_9).

The initial state of the model is determined by the axiom ω. The value of the parameter to module N sets the current cycle number to 1. The initial structure consists of a single internode I terminated by an apex A. The message type indicates the presence of a basipetal message ($m = 2$) which triggers the application of productions p_1 and p_2, initiating the first full developmental cycle. The state of the structure after 35 derivation steps (completion of the fifth developmental cycle) is shown in Figure 15.

A remarkable feature of Borchert and Honda's model is its ability to simulate the response of a plant to its environment. Specifically, after a branch has been pruned, the model redirects the fluxes to the remaining branches and accelerates their growth to compensate for the loss. A sequence of structures that illustrates this phenomenon is shown in Figure 16. In accordance with [52], the L-system used in this case extends L-system (17) with parameters and productions needed to capture the effect of aging. Consequently, a branch that was unable to grow for a given number of developmental cycles dies: it loses the ability to develop further and stops taking any fluxes.

Similar behavior is shown in Figure 17. In this case, two structures representing the shoot and the root of a plant are generated simultaneously. The flux penetrating the root at the beginning of a developmental cycle is assumed to be proportional

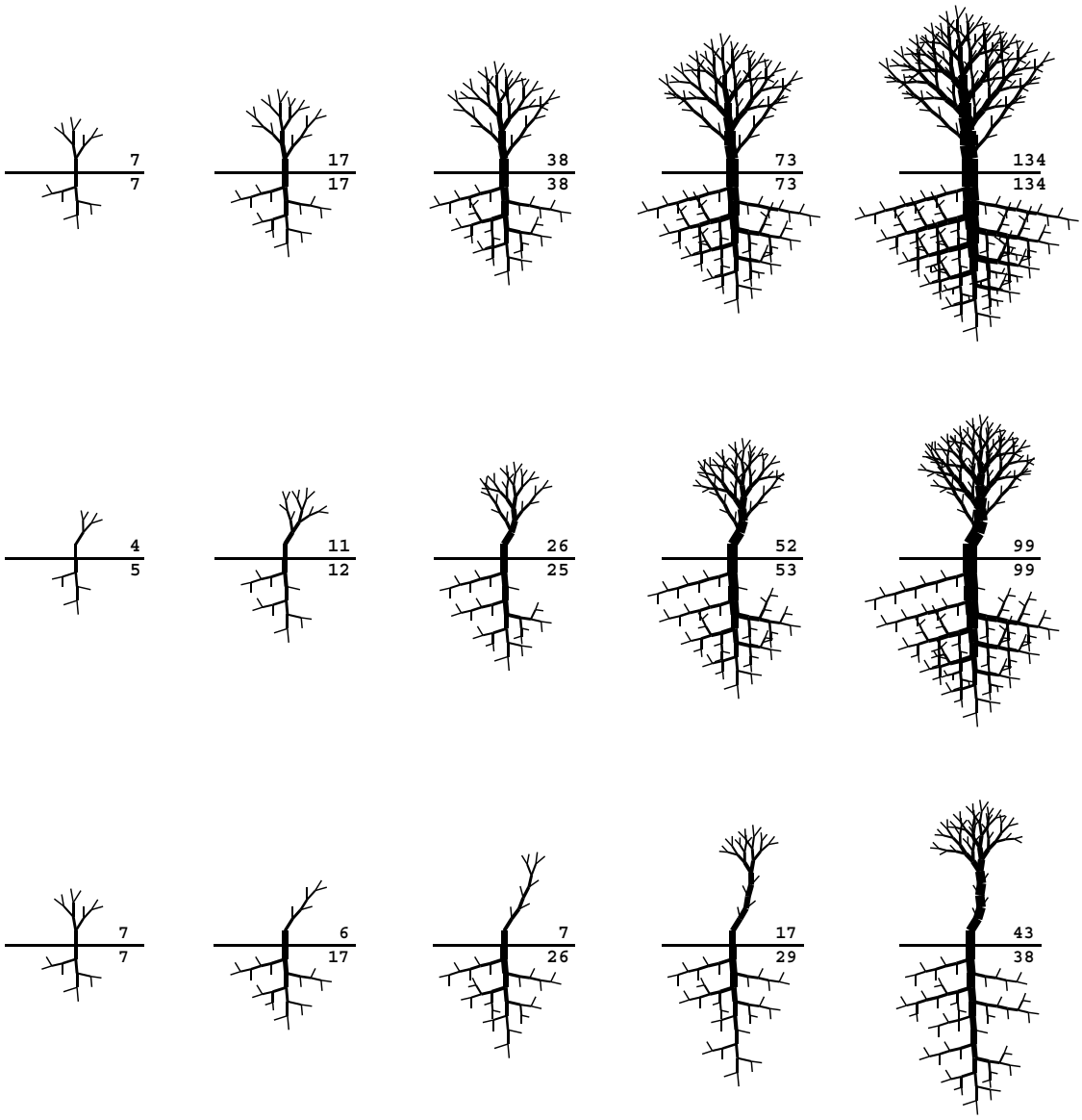

Figure 17: Application of the Borchert and Honda's model to the simulation of a complete plant, showing development unaffected by pruning (top row), affected by pruning during the third cycle of development (middle row), and affected by pruning during the fifth cycle of development (bottom row). The numbers of live apices in the shoot and root are indicated above and below the ground level. The numbers at the base of the figure indicate the number of completed developmental cycles.

to the number of apices in the shoot; reciprocally, the flux penetrating the shoot is proportional to the number of apices in the root. These assumptions form a crude approximation of plant physiology, whereby the photosynthates produced by the shoot fuel the development of the root, and water and mineral compounds gathered by the root are required for the development of the shoot. The model also assumes an increase of internode width over time and a gradual rotation of a lateral segment to the straight segment position, after the straight segment has been lost. The developmental sequence shown in the top row of Figure 17 is unaffected by pruning. The shoot and the root develop in concert. The next two rows illustrate development affected by a loss of branches. The removal of a shoot branch slows down the development of the root; on the other hand, the large size of the root, compared to the remaining shoot, fuels a fast re-growth of the shoot. Eventually, the plant is able to redress the balance between the size of the shoot and the root. This is a non-obvious consequence of the model, which illustrates the usefulness of L-systems in predicting the global behavior of plants, given the specification of their components.

8. Conclusions

L-system models integrate local processes, taking place at the level of individual modules, into developmental patterns and structures of entire plants. Consequently, they address the central problem of morphogenesis: the description and understanding of mechanisms through which living organisms acquire their form. This aspect of modeling motivated the original biological applications of L-systems investigated by Lindenmayer and his collaborators, and continues to play a key role in current biological research using L-systems. The emergence of global forms and developmental patterns is also important in the application of L-systems to computer graphics, because it makes it possible to create realistic representations of growing plants using relatively easy to specify, compact sets of data.

In principle, the mathematical formulation of L-systems should also make it possible to address biologically relevant questions in the form of a deductive theory of plant development. The results of this theory could be potentially more general than simulations, which are inherently limited to case studies. Unfortunately, construction of such a theory still seems quite remote. One reason is the lack of a precise mathematical description of plant form. This is not of crucial importance in simulations, where the results are evaluated visually, but impedes the formulation of theorems and proofs. Another difficulty is the discrepancy between studies on the theory of L-systems and the needs of biological modeling. Most theoretical results are pertinent to non-parametric 0L-systems that operate on non-branching strings without geometric interpretation (for examples, see [29]). In contrast, L-system models of biological phenomena often involve parameters, interactions between modules, and geometric features of the modeled structures. We hope that further development of the theory of L-systems will bridge this gap.

9. Acknowledgements

An overview of L-systems was the subject of several invited lectures and tutorials presented recently by P. Prusinkiewicz. Consequently, this paper includes sections of previous surveys [53,54], and coincides with [55]. The idea of using L-systems to simulate the interaction between plants and insects was proposed by Peter Room. The reported research has been sponsored by grants and graduate scholarships from the Natural Sciences and Engineering Council of Canada.

10. References

1. A. Lindenmayer. *Mathematical models for cellular interaction in development, Parts I and II.* **Journal of Theoretical Biology**, 18:280–315, 1968.
2. A. R. Smith. *Plants, fractals, and formal languages.* Proceedings of SIGGRAPH '84 (Minneapolis, Minnesota, July 22–27, 1984) in **Computer Graphics**, 18, 3 (July 1984), pages 1–10, ACM SIGGRAPH, New York, 1984.
3. P. Prusinkiewicz. *Graphical applications of L-systems.* In **Proceedings of Graphics Interface '86 — Vision Interface '86**, pages 247–253, 1986.
4. A. L. Szilard and R. E. Quinton. *An interpretation for DOL systems by computer graphics.* **The Science Terrapin**, 4:8–13, 1979.
5. J. S. Hanan. *Parametric L-systems and their application to the modelling and visualization of plants.* PhD thesis, University of Regina, June 1992.
6. P. Prusinkiewicz and A. Lindenmayer. **The algorithmic beauty of plants**. Springer-Verlag, New York, 1990. With J. S. Hanan, F. D. Fracchia, D. R. Fowler, M. J. M. de Boer, and L. Mercer.
7. P. Prusinkiewicz and J. Hanan. *Lindenmayer systems, fractals, and plants*, volume 79 of **Lecture Notes in Biomathematics**. Springer-Verlag, Berlin, 1989.
8. R. Měch and P. Prusinkiewicz. *Visual models of plants interacting with their environment.* **Proceedings of SIGGRAPH '96** (New Orleans, Louisiana, August 4–9, 1996) ACM SIGGRAPH, New York, 1996. To appear.
9. P. Prusinkiewicz, M. James, and R. Měch. *Synthetic topiary.* **Proceedings of SIGGRAPH '94** (Orlando, Florida, July 24–29, 1994), pages 351–358, ACM SIGGRAPH, New York, 1994.
10. P. Prusinkiewicz, W. Remphrey, C. Davidson, and M. Hammel. *Modeling the architecture of expanding* Fraxinus pennsylvanica *shoots using L-systems.* **Canadian Journal of Botany**, 72:701–714, 1994.
11. P. M. Room, J. S. Hanan, and P. Prusinkiewicz. *Virtual plants: new perspectives for ecologists, pathologists, and agricultural scientists.* **Trends in Plant Science**, 1(1), 1996.
12. A. Lindenmayer. *Developmental algorithms: Lineage versus interactive control mechanisms.* In S. Subtelny and P. B. Green, editors, **Developmental**

order: Its origin and regulation, pages 219–245. Alan R. Liss, New York, 1982.

13. A. Lindenmayer. *Developmental systems without cellular interaction, their languages and grammars.* **Journal of Theoretical Biology**, 30:455–484, 1971.
14. D. Frijters and A. Lindenmayer. *A model for the growth and flowering of* Aster novae-angliae *on the basis of table (1,0)L-systems.* In G. Rozenberg and A. Salomaa, editors, **L Systems**, Lecture Notes in Computer Science 15, pages 24–52. Springer-Verlag, Berlin, 1974.
15. D. Frijters and A. Lindenmayer. *Developmental descriptions of branching patterns with paracladial relationships.* In A. Lindenmayer and G. Rozenberg, editors, **Automata, languages, development**, pages 57–73. North-Holland, Amsterdam, 1976.
16. A. Bell. **Plant form: An illustrated guide to flowering plants.** Oxford University Press, Oxford, 1991.
17. J. L. Harper and A. D. Bell. *The population dynamics of growth forms in organisms with modular construction.* In R. M. Anderson, B. D. Turner, and L. R. Taylor, editors, **Population dynamics**, pages 29–52. Blackwell, Oxford, 1979.
18. D. M. Waller and D. A. Steingraeber. *Branching and modular growth: Theoretical models and empirical patterns.* In J. B. C. Jackson and L. W. Buss, editors, **Population biology and evolution of clonal organisms**, pages 225–257. Yale University Press, New Haven, 1985.
19. M. J. M. de Boer. *Analysis and computer generation of division patterns in cell layers using developmental algorithms.* PhD thesis, University of Utrecht, 1989.
20. M. J. M. de Boer, F. D. Fracchia, and P. Prusinkiewicz. *A model for cellular development in morphogenetic fields.* In G. Rozenberg and A. Salomaa, editors, **Lindenmayer systems: Impacts on theoretical computer science, computer graphics, and developmental biology**, pages 351–370. Springer-Verlag, Berlin, 1992.
21. F. D. Fracchia, P. Prusinkiewicz, and M. J. M. de Boer. *Animation of the development of multicellular structures.* In N. Magnenat-Thalmann and D. Thalmann, editors, **Computer Animation '90**, pages 3–18, Tokyo, 1990. Springer-Verlag.
22. B. B. Mandelbrot. **The fractal geometry of nature**. W. H. Freeman, San Francisco, 1982.
23. A. Lindenmayer. *Developmental algorithms for multicellular organisms: A survey of L-systems.* **Journal of Theoretical Biology**, 54:3–22, 1975.
24. A. Lindenmayer. *Algorithms for plant morphogenesis.* In R. Sattler, editor, **Theoretical plant morphology**, pages 37–81. Leiden University Press, The Hague, 1978.
25. A. Lindenmayer. *Models for multicellular development: Characterization, inference and complexity of L-systems.* In A. Kelemenová and J. Kelemen,

editors, **Trends, techniques and problems in theoretical computer science**, Lecture Notes in Computer Science 281, pages 138–168. Springer-Verlag, Berlin, 1987.

26. A. Lindenmayer and H. Jürgensen. *Grammars of development: Discrete-state models for growth, differentiation and gene expression in modular organisms.* In G. Rozenberg and A. Salomaa, editors, **Lindenmayer systems: Impacts on theoretical computer science, computer graphics, and developmental biology**, pages 3–21. Springer-Verlag, Berlin, 1992.
27. A. Lindenmayer and P. Prusinkiewicz. *Developmental models of multicellular organisms: A computer graphics perspective.* In C. G. Langton, editor, **Artificial Life**, pages 221–249. Addison-Wesley, Redwood City, 1988.
28. G. T. Herman and G. Rozenberg. **Developmental systems and languages.** North-Holland, Amsterdam, 1975.
29. G. Rozenberg and A. Salomaa. **The mathematical theory of L systems.** Academic Press, New York, 1980.
30. A. Salomaa. **Formal languages.** Academic Press, New York, 1973.
31. P. Prusinkiewicz and J. Hanan. *Visualization of botanical structures and processes using parametric L-systems.* In D. Thalmann, editor, **Scientific visualization and graphics simulation**, pages 183–201. J. Wiley & Sons, Chichester, 1990.
32. P. Prusinkiewicz and J. Hanan. *L-systems: From formalism to programming languages.* In G. Rozenberg and A. Salomaa, editors, **Lindenmayer systems: Impacts on theoretical computer science, computer graphics, and developmental biology**, pages 193–211. Springer-Verlag, Berlin, 1992.
33. B. W. Kernighan and D. M. Ritchie. **The C programming language. Second edition.** Prentice Hall, Englewood Cliffs, 1988.
34. P. Prusinkiewicz. *Applications of L-systems to computer imagery.* In H. Ehrig, M. Nagl, A. Rosenfeld, and G. Rozenberg, editors, **Graph grammars and their application to computer science; Third International Workshop**, pages 534–548. Springer-Verlag, Berlin, 1987. Lecture Notes in Computer Science 291.
35. J. S. Hanan. *PLANTWORKS: A software system for realistic plant modelling.* Master's thesis, University of Regina, 1988.
36. M. James, J. Hanan, and P. Prusinkiewicz. **CPFG version 2.0 user's manual.** Manuscript, Department of Computer Science, The University of Calgary, 1993, 50 pages.
37. H. Abelson and A. A. diSessa. **Turtle geometry**. M.I.T. Press, Cambridge, 1982.
38. S. Papert. **Mindstorms: Children, computers and powerful ideas**. Basic Books, New York, 1980.
39. J. D. Foley and A. Van Dam. **Fundamentals of interactive computer graphics**. Addison-Wesley, Reading, 1982.
40. P. Prusinkiewicz, A. Lindenmayer, and F. D. Fracchia. *Synthesis of space-filling curves on the square grid.* In H.-O. Peitgen, J. M. Henriques, and

L. F. Penedo, editors, **Fractals in the fundamental and applied sciences**, pages 341–366. North-Holland, Amsterdam, 1991.

41. H. von Koch. *Une méthode géométrique élémentaire pour l'étude de certaines questions de la théorie des courbes planes.* **Acta Mathematica**, 30:145–174, 1905.
42. D. M. Raup. *Geometric analysis of shell coiling: general problems.* **Journal of Paleontology**, 40:1178–1190, 1966.
43. D. M. Raup and A. Michelson. *Theoretical morphology of the coiled shell.* **Science**, 147:1294–1295, 1965.
44. H. Honda. *Description of the form of trees by the parameters of the tree-like body: Effects of the branching angle and the branch length on the shape of the tree-like body.* **Journal of Theoretical Biology**, 31:331–338, 1971.
45. N. Macdonald. **Trees and networks in biological models.** J. Wiley & Sons, New York, 1983.
46. P. Prusinkiewicz and L. Kari. *Subapical bracketed L-systems.* To appear in the **Proceedings of the Fifth International Workshop on Graph Grammars and their Application to Computer Science**, Williamsburg, 1994.
47. J. Lück, H. B. Lück, and M. Bakkali. *A comprehensive model for acrotonic, mesotonic, and basitonic branching in plants.* **Acta Biotheoretica**, 38:257–288, 1990.
48. P. Prusinkiewicz. *Visual models of morphogenesis.* **Artificial Life**, 1:61–74, 1994.
49. J. M. Janssen and A. Lindenmayer. *Models for the control of branch positions and flowering sequences of capitula in* Mycelis muralis *(L.) Dumont (Compositae).* **New Phytologist**, 105:191–220, 1987.
50. A. Lindenmayer. *Positional and temporal control mechanisms in inflorescence development.* In P. W. Barlow and D. J. Carr, editors, **Positional controls in plant development**. University Press, Cambridge, 1984.
51. P. M. Room, L. Maillette, and J. Hanan. *Module and metamer dynamics and virtual plants.* **Advances in Ecological Research**, 25:105–157, 1994.
52. R. Borchert and H. Honda. *Control of development in the bifurcating branch system of* Tabebuia rosea*: A computer simulation.* **Botanical Gazette**, 145(2):184–195, 1984.
53. P. Prusinkiewicz, M. Hammel, J. Hanan, and R. Měch. *Visual models of plant development.* In G. Rozenberg and A. Salomaa, editors, **Handbook of formal languages**. Springer-Verlag, Berlin, 1996. To appear.
54. P. Prusinkiewicz, M. Hammel, R. Měch, and J. Hanan. *The artificial life of plants.* In D. Terzopoulos, editor, **SIGGRAPH 1995 course notes on Artificial Life**, pages 1–1 – 1–38. ACM SIGGRAPH, 1995.
55. P. Prusinkiewicz, M. Hammel, J. Hanan, and R. Měch. *L-systems: from the theory to visual models of plants.* **Machine Graphics and Vision**, 5(1/2):365–392, 1996.